



# Convergence of an S-Wave Calculation of the He Ground State

J. Mitroy, M.W.J. Bromley and K. Ratnavelu

December 2006

Publication Number: CSRCR2006-31

Computational Science &  
Engineering Faculty and Students  
Research Articles

Database Powered by the  
Computational Science Research Center  
Computing Group

## COMPUTATIONAL SCIENCE & ENGINEERING



**SAN DIEGO STATE  
UNIVERSITY**

Computational Science Research Center  
College of Sciences  
5500 Campanile Drive  
San Diego, CA 92182-1245  
(619) 594-3430



J.Mitroy\*

*Faculty of Technology, Charles Darwin University, Darwin NT 0909, Australia*

M.W.J.Bromley

*Department of Physics, San Diego State University, San Diego CA 92182, USA<sup>†</sup>*

K. Ratnavelu<sup>‡</sup>

*Faculty of Science, Universiti Malaya, 50603 Kuala Lumpur, Malaysia*

(Dated: July 12, 2006)

The Configuration Interaction (CI) method using a large Laguerre basis restricted to  $\ell = 0$  orbitals is applied to the calculation of the He ground state. The maximum number of orbitals included was 60. The numerical evidence suggests that the energy converges as  $\Delta E^N \approx A/N^{7/2} + B/N^{8/2} + \dots$  where  $N$  is the number of Laguerre basis functions. The electron-electron  $\delta$ -function expectation converges as  $\Delta \delta^N \approx A/N^{5/2} + B/N^{6/2} + \dots$  and the variational limit for the  $\ell = 0$  basis is estimated as  $0.1557637174(2) a_0^3$ . It was seen that extrapolation of the energy to the variational limit is dependent upon the basis dimension at which the exponent in the Laguerre basis was optimized. In effect, it may be best to choose a non-optimal exponent if one wishes to extrapolate to the variational limit. An investigation of the Natural Orbital asymptotics revealed the energy converged as  $\Delta E^N \approx A/N^6 + B/N^7 + \dots$  while the electron-electron  $\delta$ -function expectation converged as  $\Delta \delta^N \approx A/N^4 + B/N^5 + \dots$ . The asymptotics of expectation values other than the energy showed fluctuations that depended on whether  $N$  was even or odd.

PACS numbers: 31.10.+z, 31.15.Pf, 31.25.Eb

## I. INTRODUCTION

There have been a number of studies of the convergence of the configuration interaction (CI) expansion of the helium ground state [1–8] following the pioneering work of Schwartz [9]. These studies have investigated the convergence of the energy with respect to the number of partial waves included in the wave function and also with respect to the dimension of the radial basis.

It has been known since 1962 [9] that the energy converges slowly with respect to  $J$ , the maximum angular momentum of any orbital included in the CI expansion. In particular the leading term to the energy increment is known to behave as

$$\Delta E^J = \langle E \rangle^J - \langle E \rangle^{J-1} \sim \frac{A_E}{(J + \frac{1}{2})^4} \quad (1)$$

at high  $J$ . Later work [1–4, 6] showed that the energy increments can be written more generally as

$$\Delta E^J = \frac{A_E}{(J + \frac{1}{2})^4} + \frac{B_E}{(J + \frac{1}{2})^5} + \frac{C_E}{(J + \frac{1}{2})^6} + \dots, \quad (2)$$

where explicit expressions for  $A_E$  and  $B_E$  exist, namely

$$A_E = -6\pi^2 \int |\Psi(r, r, 0)|^2 r^5 dr = -0.074226 \quad (3)$$

$$B_E = -\frac{48\pi}{5} \int |\Psi(r, r, 0)|^2 r^6 dr = -0.030989. \quad (4)$$

No expressions for  $C_E$  exist. The numerical values in eqs. (3) and (4) are obtained from close to exact wave functions [2].

However, the convergence with respect to  $J$  represents only one aspect of the convergence problem. Just as important is the convergence with respect to the dimension of the radial basis  $N$ , for a given  $J$ . How do the increments to  $E$  with increasing  $N$

$$\begin{aligned} \Delta E^N &= \langle E \rangle^N - \langle E \rangle^{N-1} \\ &\sim \frac{A'_E}{N^p} + \frac{B'_E}{N^{p+t}} + \frac{C'_E}{N^{p+2t}} + \dots, \end{aligned} \quad (5)$$

behave? In effect, what are the values of  $p$  and  $t$ ? This aspect of the CI expansion is not as well understood as the convergence with  $J$  and there have been no studies equivalent in sophistication to those of Schwartz [9], Hill [2] and Kutzelnigg and collaborators [3, 6]. Some attention has been given to the radial convergence of the hydrogen atom in gaussian basis sets [10]. The seminal investigation of Carroll and collaborators concluded that  $p \approx 6$  for a natural orbital (NO) basis [1, 11]. This result has been quite influential, and can be regarded as ultimately motivating the use of principal quantum number

\*Electronic address: jxm107@rsphysse.anu.edu.au

<sup>†</sup>Electronic address: mbromley@physics.sdsu.edu

<sup>‡</sup>Electronic address: kuru052001@gmail.com

expansions to extrapolate energies to the infinite basis limit from correlation consistent basis sets [12]. More recently, Goldman performed a regression analysis to give  $p \approx 5.7$  for a NO basis and  $p \approx 3.8$  for a Slater basis with a common exponent [13].

The radial basis sets used for the configuration interaction or many body perturbation theory treatments of atomic structure can be broadly divided into two classes. In the first class, one defines a box and a piece-wise polynomial (e.g a spline) is used to define the radial dependence of the wave function in the interior of the box. The properties of the radial basis are determined by the size of the box, the number of knot points, and where they are located. The other approach typically expands the wave function in terms of a basis of functions with a convenient analytic form, examples would be an evenly tempered set of Slater type orbitals (STOs) [3, 7] (this type of basis set is often optimized with respect to a couple of parameters used to defined a sequence of exponents) or a set of Laguerre type orbitals (LTOs) [14–16].

The two most recent examples of these two approaches are the calculations by Decleva *et al* (B-splines) [4] and Sims and Hagstrom (Slater basis) [7] which are the biggest calculations of their respective type. The B-spline calculation has given estimates  $\Delta E^J$  increments that are believed to be accurate to within  $10^{-8}$  hartree or better. One of the reasons this accuracy is possible is that  $\Delta E^J$  varies smoothly as the number of knot points is adjusted. This made it possible to obtain reasonable estimates of the infinite basis limit. Their estimate of the  $s$ -wave limit was accurate to better than  $10^{-9}$  hartree. Achieving this extreme level of accuracy was not possible when using the Slater basis [7] since linear dependence issues made it problematic to expand their radial basis to completeness. Indeed, resorting to REAL\*24 arithmetic still resulted in an error of  $4 \times 10^{-6}$  hartree.

In some investigations of the convergence properties of the CI expansion for the helium atom [8] and mixed electron-positron systems [17] it became apparent that a better understanding of the issues that influence the convergence of the radial basis was desirable. For example, it was apparent that the dimension of the radial basis should be increased as  $J$  increases in order to ensure the successive  $\Delta E^J$  increments are computed to the same relative accuracy [8, 17, 18]. In addition, it was readily apparent that extrapolation of the radial LTO basis to the  $N \rightarrow \infty$  limit was not straightforward.

In this work, we investigate the radial convergence of the CI expansion for a more manageable model of the helium atom with the orbitals restricted to the  $\ell = 0$  partial wave. The linear dependence issues that are such a problem for a Slater basis are eliminated by choosing the radial basis to consist of LTOs [15, 19], (formally, the LTO basis spans the same space as the common exponent Slater basis, i.e.  $r^{n_i} \exp(-\lambda r)$ ). We note in passing the previous work of Holooin [16] who also investigated the convergence of an LTO basis for an  $s$ -wave of helium. Initially, we examine the merits of using an LTO

basis with the exponent optimized to the basis dimension. Then the nature of the asymptotic expansion for the energy increments is deduced. Finally, the density matrix for our best wave function is diagonalized and the convergence properties of the natural orbital expansion are also determined. As part of this analysis, attention is also given to the convergence of the electron-electron coalescence matrix element since it arises in calculations of the two-electron relativistic Darwin correction [20] and electron-positron annihilation [21].

## II. THE $s$ -WAVE ENERGY FOR HELIUM

The non-relativistic hamiltonian for the  $^1S^e$  ground state of helium

$$H = - \sum_{i=1}^{N_e} \left( \frac{1}{2} \nabla_i^2 + \frac{2}{r_i} \right) + \frac{1}{r_{12}}, \quad (6)$$

is diagonalized in a basis consisting of anti-symmetric products of single electron orbitals

$$|\Psi; S=0\rangle = \sum_{i,j} c_{ij} \mathcal{A}_{12} \langle \frac{1}{2} \mu_i \frac{1}{2} \mu_j | 00 \rangle \phi_i(\mathbf{r}_1) \phi_j(\mathbf{r}_2). \quad (7)$$

The functions  $\phi(\mathbf{r})$  are single electron orbitals Laguerre functions with the radial form

$$\chi_\alpha(r) = N_\alpha r^\ell \exp(-\lambda_\alpha r) L_{n_\alpha - \ell - 1}^{(2\ell+2)}(2\lambda_\alpha r), \quad (8)$$

where the normalization constant is

$$N_\alpha = \sqrt{\frac{(2\lambda_\alpha)(n_\alpha - \ell - 1)!}{(\ell + n_\alpha + 1)!}}. \quad (9)$$

The function  $L_{n_\alpha - \ell - 1}^{(2\ell+2)}(2\lambda_\alpha r)$  is an associated Laguerre polynomial that can be defined in terms of a confluent hypergeometric function [15, 22, 23]. In the present work  $\ell$  is set to zero. The basis can be characterized by two parameters,  $N$ , the number of LTOs, and  $\lambda$  the exponent characterizing the range of the LTOs. It is normal to use a common exponent,  $\lambda$  and when this is done the basis functions form an orthogonal set. The exponent can be optimized to give the lowest energy and when this is done one can define  $\lambda_M$  to be the value of optimal  $\lambda$  for a basis of dimension  $M$ . The value of  $\lambda_M$  was seen to increase  $M$  increased.

Calculations for basis sets with  $\lambda_M$  optimized for dimensions of 10, 20, 30, 40, 50 and 60 have been performed. The optimal exponents are listed in Table I along with the energy for those values of  $M$ . The calculations were expedited by using the result that the two-electron Slater integrals for any  $\lambda$  are related to each other by a very simple scaling relation. Accordingly, the list of Slater integrals could be generated once (by numerical integration using gaussian quadrature [15]) for a given  $\lambda$ , and then recycled by rescaling for calculations at different  $\lambda$  (refer to Appendix B). Calculations with  $N$  ranging from 1 to 60 have been performed for the six values

TABLE I: Comparison of different CI calculations of the  $s$ -wave model of the He atom ground state. The expectation value of the electron-electron  $\delta$ -function (in  $a_0^3$ ) is denoted as  $\langle\delta\rangle$ . The data in the  $\langle E\rangle^M$  and  $\langle E\rangle^{60}$  columns are the energies (in hartree) with  $N = M$  and  $N = 60$  basis sets respectively. The data in the  $\langle E\rangle^\infty$  and  $\langle\delta\rangle^\infty$  columns are obtained by doing an explicit calculations with  $N = 60$  and then adding in the  $60 \rightarrow \infty$  correction assuming an  $A/N^{-p}$  asymptotic form.

$M$	$\lambda_M$	$\langle E\rangle^M$	$\langle E\rangle^{60}$	$\langle E\rangle^\infty$	$\langle\delta\rangle^M$	$\langle\delta\rangle^\infty$
10	3.07	-2.879 022 691 296	-2.879 028 727 964	-2.879 028 7667	0.155 922 600 334	0.155 763 879
20	4.80	-2.879 028 507 141	-2.879 028 754 899	-2.879 028 7671	0.155 789 345 524	0.155 763 796
30	6.45	-2.879 028 726 601	-2.879 028 761 447	-2.879 028 7672	0.155 772 304 341	0.155 763 771
40	8.04	-2.879 028 756 467	-2.879 028 763 935	-2.879 028 7673	0.155 767 637 040	0.155 763 760
50	9.57	-2.879 028 763 441	-2.879 028 765 118	-2.879 028 7670	0.155 765 847 239	0.155 763 757
60	11.10	-2.879 028 765 650	-2.879 028 765 650	-2.879 028 7661	0.155 765 002 122	0.155 763 860
Decleva <i>et al</i> [4]			-2.879 028 767 289			
Goldman <i>et al</i> [13]			-2.879 028 767 319			

of  $\lambda_M$  listed in Table I. The dimension of the hamiltonian for the largest calculation was 1830. The quantities listed in the tables and the text are given in atomic units. The most precise energy for the helium  $s$ -wave model is that of Goldman [13, 24] who used a basis written in terms of  $r_<, r_>$  co-ordinates to obtain an energy of  $E = -2.879028767319214$  hartree.

### A. Use of quadruple precision arithmetic

The present calculations were all performed with quadruple precision arithmetic. It was only possible to get energies precise to 13 significant digits for the largest calculations when double precision arithmetic was used. This was caused by roundoff error gradually accumulating during the course of the rather extensive calculations and the 13 digits appears to be the limit that can be achieved for double precision arithmetic (some experimentation revealed that the last 2 digits of the 15 double precision digits were sensitive to different Fortran compilers and even the optimization options of those compilers). The analysis requires investigation of the energy differences of eq. (5), and these energy differences can be rather small (e.g.  $\Delta E^{60} = 1.5 \times 10^{-10}$  hartree for the  $\lambda_{60}$  basis). The fluctuations caused by roundoff did have a noticeable impact on the parameters derived from these energy differences at large  $N$ . These fluctuations were removed once quadruple precision arithmetic was adopted.

### III. SIMPLE POWER LAW DECAY

All observable quantities can be defined symbolically as

$$\langle X \rangle^N = \sum_{n=1}^N \Delta X^n, \quad (10)$$

where  $\Delta X^n$  is the increment to the observable that occurs when the basis dimension is increased from  $n-1$  to  $n$ , e.g.

$$\Delta X^n = \langle X \rangle^n - \langle X \rangle^{n-1}. \quad (11)$$

Hence, one can express the limiting value formally as

$$\langle X \rangle = \langle X \rangle^N + \sum_{n=N+1}^{\infty} \Delta X^n. \quad (12)$$

The first term on the right hand side will be determined by explicit computation while the second term will be estimated. Obtaining an estimate of the remainder term does require some qualitative knowledge of how the  $\Delta X^N$  terms decay with  $N$ . For example, previous computational investigations indicate that the natural orbital decomposition leads to a  $\Delta E^N \approx N^{-6}$  dependence [1, 25]. As far as we know, there have not been any detailed investigations of the  $N$  dependence of a Laguerre basis.

A useful way to analyze the convergence is to assume the increments obey a power law decay of the form

$$\Delta X^N \sim \frac{A_X}{N^p}, \quad (13)$$

and then determine the value of  $p$  from two successive values of  $\Delta X$  using

$$p = \ln \left( \frac{\Delta X^{N-1}}{\Delta X^N} \right) / \ln \left( \frac{N}{N-1} \right). \quad (14)$$

Figure 1 plots the exponent derived from the energy increments for six different values of  $\lambda_M$ . The succession of curves show that  $p_E$  tends to peak at values larger than 10 at an intermediate  $N$  and then shows a tendency to decrease. The value at  $N = 60$  was  $p_E \approx 3.7$  for the most of the curves shown in figure 1.

The salient point to be extracted from Figure 1 is that the value of  $p_E$  for a given  $\lambda_M$  at  $N = M$  is quite different from the asymptotic value, e.g. the value of  $p_E$  for the  $\lambda_{20}$  curve is much larger at  $N = 20$  than it is

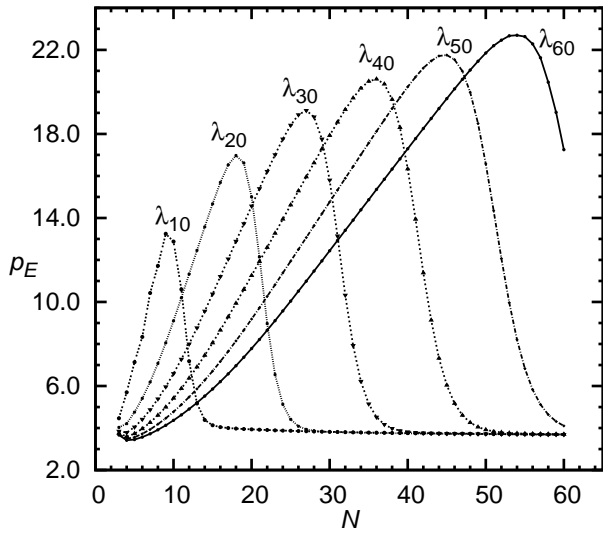


FIG. 1: The exponents  $p_E$  as a function of  $N$  for the  $s$ -wave calculations of the He ground state. The different curves were obtained from the LTO basis sets with the exponents listed in Table I.

at  $N = 60$ . This is quite an annoying result. Ideally, one would like to perform the largest calculation with the exponent optimized for that dimension basis. Then the specific form of the power law decay would be estimated by analyzing the energies obtained from a series of slightly smaller calculations. This information would subsequently be used to estimate the energy or other expectation value in the variational limit. However, this is not possible since the energy increments will not have achieved their asymptotic form.

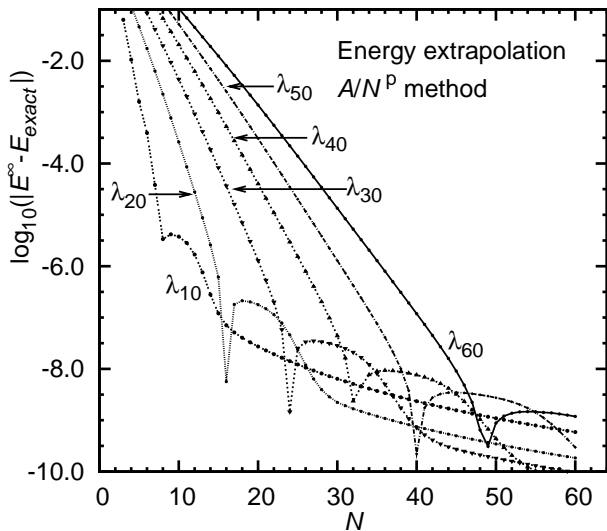


FIG. 2: The extrapolated  $N \rightarrow \infty$  limit for the He ground state energy for different values of  $\lambda_M$ . The exact  $s$ -wave energy is taken from the  $J = 0$  calculation of Goldman [13].

Although there are problems in using an optimized exponent, it may still be possible to analyze a sequence of energies from a calculation with a non-optimized exponent and thereby estimate the variational limit. Assuming that the increments obey eq. (13), one can write

$$A_X = N^p \Delta X^N, \quad (15)$$

and thus the  $n > N$  remainder term

$$\sum_{n=N+1}^{\infty} \frac{A_X}{N^p} \approx \frac{A_X}{(p-1)(N+\frac{1}{2})^{p-1}}. \quad (16)$$

can be derived from  $\langle X \rangle^{N-2}$ ,  $\langle X \rangle^{N-1}$  and  $\langle X \rangle^N$  [8, 17]. When this remainder was evaluated in this work, the first 10000 terms of the sum over  $n$  were computed explicitly. Then the approximate relation eq. (16) was used.

Figure 2 shows the estimated variational limit as a function of  $N$  for the  $\lambda_i$  listed in Table I. An explicit calculation including  $N$  LTOs was initially performed to determine  $\langle E \rangle^N$ . Then eq. (16) was used to estimate the remainder and hence deduce the variational limit. The variational limits in Table I were extracted from the calculations with  $N = 60$ . The exact variational limit can be predicted to the 9th digit after the decimal point. The most inaccurate estimate of the variational limit is that from the  $\lambda_{60}$  calculation. So the calculation that is explicitly optimized at  $N = 60$ , (i.e. with  $\lambda_{60}$ ), and gives the best energy at  $N = 60$ , gives the worst estimate of the variational limit!

A CI calculation of the  $\text{Li}^+$  ground state restricted to the  $\ell = 0$  partial wave was also performed to check whether the conclusions above were peculiar to He. Once again, the exponent  $p_E$  was approximately 3.7 at  $N = 60$  and the convergence pattern for  $N < M$  was distorted by optimization of the exponent.

#### IV. THE $\delta$ -FUNCTION EXPECTATION VALUE

Part of the motivation for the present study is to gain a better understanding of how to perform CI calculations for mixed electron-positron systems. Apart from the energy, the next most important expectation value for a positronic system is the electron-positron annihilation rate [21]. The annihilation rate is proportional to the expectation of the electron-positron delta function, and has the inconvenient property that it is even more slowly convergent than the energy [15, 26]. Accordingly, the convergence of the electron-electron  $\delta$ -function is investigated using the methodology previously used for the energy. The only independent investigation of this quantity for an  $s$ -wave model of helium was by Halkier *et al* [20] who obtained  $0.155786 a_0^3$ .

Figure 3 tracks the behavior of the exponent  $p_\delta$  derived from eq. (14). It can be seen that  $p_\delta$  achieves values exceeding 10 before it decreases to its asymptotic values. The present calculations give  $p_\delta \approx 2.6$  at  $N = 60$  although  $p_\delta$  is still exhibiting a slow but steady decrease.

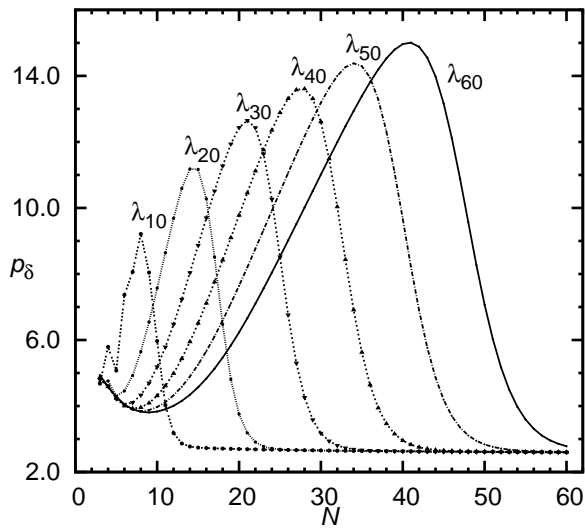


FIG. 3: The estimated exponents  $p_\delta$  as a function of  $N$  for the LTO calculations of the He ground state  $\langle \delta \rangle$ . The different curves were obtained with the LTO basis sets listed in Table I.

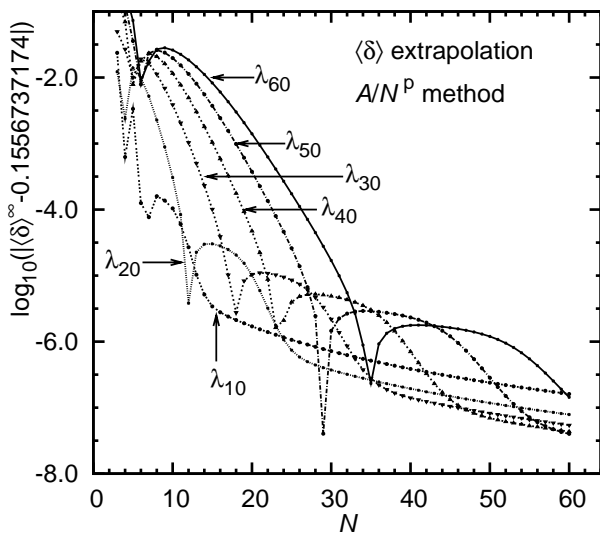


FIG. 4: The convergence of  $\langle \delta \rangle$  for the He ground state as a function of  $N$ . The absolute value of the difference of the extrapolated  $N \rightarrow \infty$  limit subtracted from  $0.1556737174 a_0^3$  is plotted.

Although distortions in the convergence pattern are still present, they are less severe than the energy since the successive  $\Delta \delta^N$  increments are larger. As a rule,  $p_\delta$  was at least 10% larger than 2.6 at  $N = M$ . A choice of  $N \geq (M+10)$  would generally lead to  $p_\delta$  being in the asymptotic region.

Figure 4 shows the estimated variational limit of  $\langle \delta \rangle^\infty$  as a function of  $N$  for the six different values of  $\lambda_M$

listed in Table I. An explicit calculation including  $N$  LTOs was initially performed, then eq. (16) was used to estimate the variational limit. A variational limit of  $\langle \delta \rangle = 0.1556737174(2) a_0^3$  (see later discussion) was assumed for plotting purposes. The notable feature is that the  $\lambda_{60}$  estimate of the limit at  $N = 60$  is one of the least accurate.

## V. A CLOSER LOOK AT THE ASYMPTOTIC POWER LAWS

Figures 5 and 6 show the behavior of the  $p_E$  and  $p_\delta$  versus  $\frac{1}{\sqrt{N}}$  for values of  $N$  greater than 16. Curves are not shown for all the  $\lambda_M$  exponents. In some cases, the values of  $p_\delta$  did not fall within the plotting window.

The notable feature to be gleaned from both set of curves is the essentially linear behavior  $p_{\text{delta}}$  with respect to  $\frac{1}{\sqrt{N}}$  for values of  $N$  greater than 16 and a visual inspection suggests that the limiting exponents is  $p_\delta = 2.5$ . The purely visual evidence that the lowest order term of  $p_E$  is  $O(N^{-1/2})$  is not as compelling as that for  $p_{\text{delta}}$ , but by analogy with this form has been assumed and subjected to extensive testing.

More substantial evidence is provided by a fit of the  $p$  vs  $N$  data to an inverse power series of the form

$$p = p_0 + \sum_{i=1}^{N_p} \frac{p_i}{\sqrt{N^i}}. \quad (17)$$

What we have done is fit  $(N_p + 1)$  successive  $p_E$  or  $p_\delta$  values to eq. (17) for the  $\lambda_{10}$  data sequence. The results of those fits are given in Table II.

Using a 4 or 5 term fits (and 6 term fit in the case of  $p_E$ ) results in limiting exponents very close to either 3.5 (for  $p_E$ ) or 2.5 (for  $p_\delta$ ). These estimates were also reasonably stable. For example, the value of  $p_E$  for a 5-term fit for a data sequence terminating at  $N = 50$  (as opposed to  $N = 60$  in Table II) was 3.4970.

The validity of the series, eq. (17) immediately suggests that the asymptotic forms for  $\Delta E^N$  are

$$\Delta E^N = \frac{A_E}{N^{7/2}} + \frac{B_E}{N^{8/2}} + \frac{C_E}{N^{9/2}} + \dots \quad (18)$$

$$\Delta \delta^N = \frac{A_\delta}{N^{5/2}} + \frac{B_\delta}{N^{6/2}} + \frac{C_\delta}{N^{7/2}} + \dots \quad (19)$$

(In Appendix A it is demonstrated that an exponent variation of  $p = p_0 + B/\sqrt{N}$  arises from an inverse power series in  $\Delta X^N$  with a leading term of  $B/N^{p_0}$  and with the power increasing by  $\sqrt{N}$  for successive terms). Although eqs. (18) and (19) are best described as a conjecture, the numerical evidence in support of the conjecture will be seen to be strong.

The applicability and utility of eqs. (18) and (19) was tested by fitting these equations to  $\langle E \rangle^N$  and  $\langle \delta \rangle^N$  values and then using eq. (16) to determine the  $N \rightarrow \infty$  limits

TABLE II: Results of using 2, 3, 4, 5 or 6 term inverse power series (corresponding to  $N_p = 1, 2, 3, 4$  and 6) to determine the limiting value of the exponents and the energy and  $\delta$ -function (in  $a_0^3$ ). The results for the LTO data sequences were taken from the largest calculations for the  $\lambda_{10}$  exponents. The results for the NO data sequences were extracted at  $N = 20$  while those for the energy optimized LTO sequence were determined at  $N = 30$ . Data entries with an asterisk, \*, were obtained using a weighted average (as described in the text) due to fluctuations depending on whether the  $N$  was even or odd.

$N_p$	$p_0$	$p_1$	$A_X$	$\langle X \rangle^\infty$
LTO data sequence: $\lambda_{10}$ basis				
$\langle E \rangle$				
1	3.4310	2.0481	-0.00182	-2.879 028 767 0519
2	3.5121	1.1301	-0.00225	-2.879 028 767 3496
3	3.4978	1.1267	-0.00212	-2.879 028 767 3154
4	3.4988	1.0958	-0.00215	-2.879 028 767 3196
5	3.5012	1.0032	-0.00215	-2.879 028 767 31920
$\langle \delta \rangle$				
1	2.4809	0.9444	-0.00535	0.155 763 7540
2	2.4975	0.6872	-0.00562	0.155 763 7156
3	2.5024	0.5760	-0.00560	0.155 763 7172
4	2.4989	0.6810	-0.00559	0.155 763 7174
NO data sequence				
$\langle E \rangle$				
1	5.9916	2.7712	-0.2959	-2.879 028 767 3054
2	5.9971	2.5553	-0.2995	-2.879 028 767 3176
3	5.9959	2.6256	-0.2996	-2.879 028 767 3177
4	5.9671	4.7513	-0.2999	-2.879 028 767 3179
$\langle \delta \rangle$				
1	3.9973	1.620*	-0.1957	0.155 763 7197
2	3.9980*	1.681*	-0.1962*	0.155 763 7177*
3	3.9997*	1.599*	-0.1963*	0.155 763 7175*
Energy optimized LTO data sequence				
$\langle E \rangle$				
1	5.6562	149.13	-1.543	-2.879 028 767 3333
$\langle \delta \rangle$				
1	3.8093*	0.3839*	-0.3879*	0.155 763 7191*

for the individual terms. Asymptotic series with up to 5-terms (i.e.  $N_p = 4$ ) were also investigated.

Figure 7 shows  $\langle E \rangle^\infty$  for the  $\lambda_{10}$  basis using the asymptotic series of different lengths to estimate the  $N \rightarrow \infty$  correction. It is noticeable that all the representations of eq. (18) exhibit better convergence properties than eq. (13) and the 6-term representation has the best convergence characteristics for  $N > 30$ . (It should be noted that the 3-, 4-, 5- and 6- term extrapolations to  $\langle E \rangle^\infty$  exhibited fluctuations of order  $10^{-5}$  to  $10^{-9}$  hartree when the calculation was performed in double precision arithmetic). The increasingly better convergence characteristics as  $N_p$  increases is consistent with eq. (18) be-

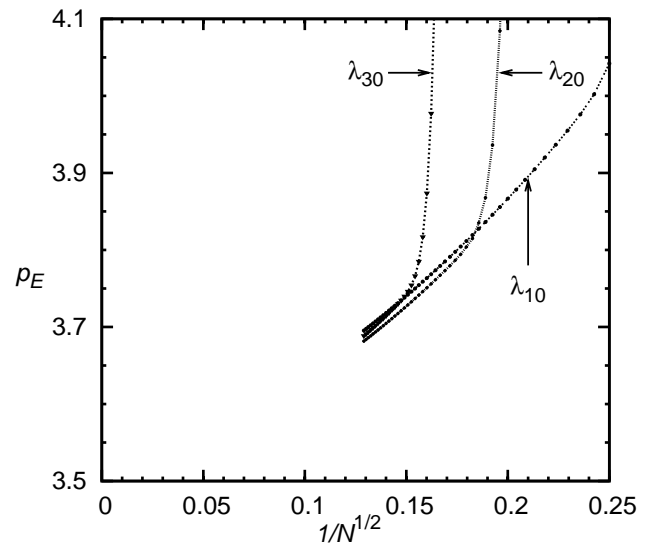


FIG. 5: The exponents  $p_E$  as a function of  $\frac{1}{\sqrt{N}}$  for the  $s$ -wave calculations of the He ground state. The different curves were obtained from the LTO basis sets with the exponents listed in Table I.

ing the asymptotic form describing the energy convergence with respect to a LTO basis. The estimated  $\langle E \rangle^\infty$  limits at  $N = 60$  for the various asymptotic expressions are given in Table II. The 6-term estimate was  $\langle E \rangle^\infty = -2.87902876731920$  hartree which agrees with the value of Goldman, namely  $E = -2.87902876731921$  by  $1 \times 10^{-14}$  hartree. The precision of the extrapolated value exceeds the precision of raw  $\langle E \rangle^{60}$  energy by a factor of 1,000,000! This improvement is best placed in perspective by noting that the  $\lambda_{10}$  calculation would have to be extended to  $N \approx 10^6$  to achieve the same level of precision.

This extreme accuracy is not reproduced if one uses other forms for the asymptotic series. For example, making the choice  $\Delta E^N = A_E/N^4 + B_E/N^5 + \dots$  results in much poorer estimates of  $\langle E \rangle^\infty$ . Using a 4-term series for the  $\lambda_{10}$  basis set for this asymptotic series gave  $\langle E \rangle^\infty = -2.879028802777$  hartree which is in error by  $3.5 \times 10^{-7}$  hartree.

The ability to accurately predict  $\langle E \rangle^\infty$  using eq. (18) has been tested for other values of  $\lambda$ . Making the choice  $\lambda = \lambda_{20}$  gave  $\langle E \rangle^\infty = -2.87902876731919$  hartree when the 6-term series was used to make the extrapolation. In summary, there is strong numerical evidence that eq. (18) correctly describes the convergence of the energy with  $N$ .

The slower convergence of the electron-electron  $\delta$ -function as  $\Delta \delta^N \approx A/N^{5/2}$  means that the ability to extrapolate to the  $N \rightarrow \infty$  limit is even more important in obtaining accurate expectation values. Figure 8 shows the  $\langle \delta \rangle^\infty$  estimates for the  $\lambda_{10}$  basis while using eq. (13) and eq. (19) to describe the large  $N$  limiting behavior. It is noticed that the convergence improved as  $N_p$  increased as long as  $N$  was sufficiently large. Choosing

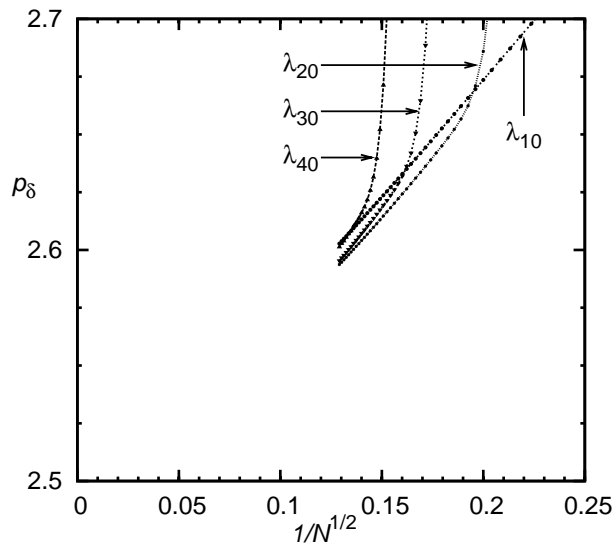


FIG. 6: The estimated exponents  $p_\delta$  as a function of  $\frac{1}{\sqrt{N}}$  for the LTO calculations of the He ground state  $\langle\delta\rangle$ . The different curves were obtained from the LTO basis sets with the exponents listed in Table I.

$N > (M + 10)$  would seem to be sufficient for 2-term or 3-term fits to eq. (19). The specific numerical estimates of  $\langle\delta\rangle^\infty$  for various extrapolations at  $N = 60$  are given in Table II. The 5-term fit gave  $\langle\delta\rangle^\infty = 0.1557637174 a_0^3$ . Given that  $\langle\delta\rangle^{60}$  for the  $\lambda_{10}$  basis was  $0.1557727974 a_0^3$ , the improvement in precision from the 5-term expansion corresponds to 4-5 orders of magnitude. This result is not specific to the  $\lambda_{10}$  basis. Usage of the  $\lambda_{20}$  basis resulted in an estimate of  $\langle\delta\rangle^\infty = 0.1557637175 a_0^3$ . Given these results it would seem reasonable to assign a value of  $0.1557637174(2) a_0^3$  to  $\langle\delta\rangle$ . This is the value that was adopted as the “exact” value when plotting Figures 4 and 8.

The more sophisticated extrapolations shown in Figure 8 exhibit even-odd fluctuations at the lower values of  $N$  and led us to omit consideration of a 6-term fit. These fluctuations are believed to arise from structural features of the helium ground state for reasons outlined in the next section.

## VI. CONVERGENCE OF A NATURAL ORBITAL BASIS

The asymptotic form of the energy for a wave function written in terms of its natural orbital decomposition [1, 11, 14] has also been re-examined for s-wave helium. First a very large calculation of the ground state wave function with a basis of 70 LTOs ( $\lambda = 11.10$ ) was performed. The one electron density matrix was then diagonalized and the resulting natural orbitals were used to define a new orbital basis ordered in terms of decreasing ground state occupancy. In its natural orbital form, the wave function

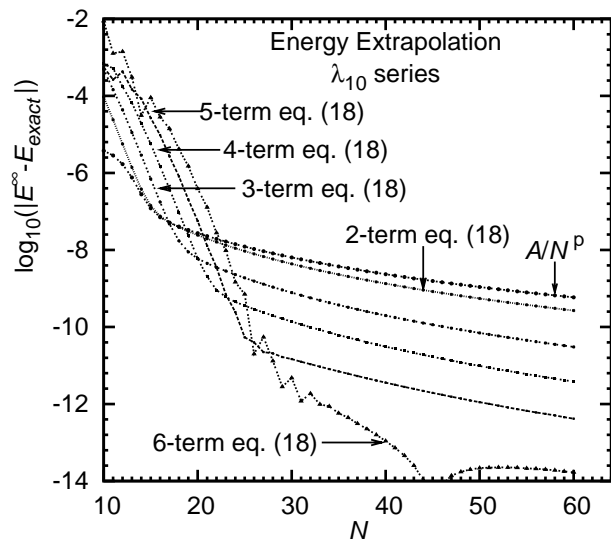


FIG. 7: The extrapolated  $N \rightarrow \infty$  limit for the He ground state energy obtained from the different asymptotic expansions. The energy sequence from the  $\lambda_{10}$  was used. The exact s-wave energy as given by the calculation of Goldman *et al* [4] is subtracted from the energy.

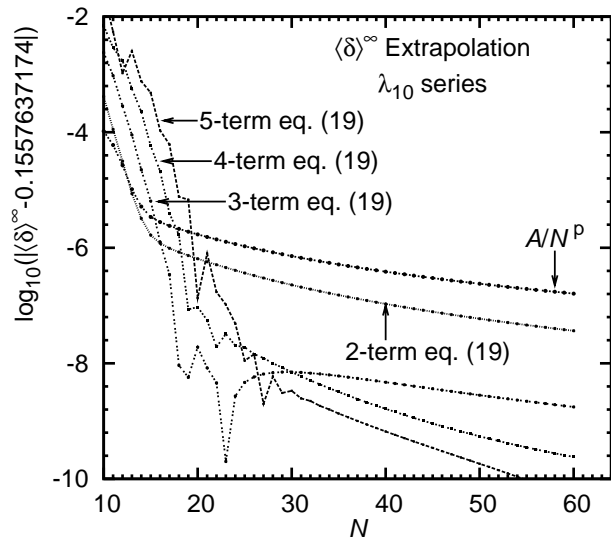


FIG. 8: The extrapolated  $N \rightarrow \infty$  limit for the He ground state  $\langle\delta\rangle^\infty$  for the different extrapolation methods applied to the  $\lambda_{10}$  basis as described in the text.

for a  $1S^e$  state is written

$$|\Psi\rangle = \sum_i d_i \mathcal{A}_{ij} \langle \frac{1}{2}\mu_i \frac{1}{2}\mu_j | 00 \rangle \phi_i(\mathbf{r}_1) \phi_j(\mathbf{r}_2). \quad (20)$$

The natural orbital expansion is usually ordered in terms of decreasing  $|d_i|$ .

Table III gives  $\langle E \rangle$  and  $\langle\delta\rangle$  for the sequence of increasingly larger NO expansions. For these calculations, the



generated NOs were added successively and  $\langle E \rangle^N$  and  $\langle \delta \rangle^N$  computed once the hamiltonian was diagonalized. The calculations were taken up to a maximum NO expansion length of 20. The LTO basis of dimension 70 was not large enough to give a precise representation of the NOs beyond that point. The energies in the table are expected to be accurate estimates of the “exact” NO energy for all digits with the possible exception of the last two. The energies in Table III are slightly lower than the previous tabulations of the  $s$ -wave NO energies by Carroll *et al* [1] and Goldman [13]. We treat the NO orbitals merely as a particularly optimal set of orbitals to input into a CI calculations. So unlike Carroll *et al* and Goldman the configuration space is not restricted to only include  $\phi_i(\mathbf{r}_1)\phi_i(\mathbf{r}_2)$  type configurations. It should be noted that we have also done some calculations using the pure NO configuration space and when this is done the energies agree with those of Carroll *et al* and Goldman to all digits. The  $\langle \delta \rangle^N$  values in Table III are expected to approximate those of the “exact” basis to about to 10 digits.

Figure 9 shows the variation of  $p_E$  and  $p_\delta$  versus  $1/N$  for a sequence of increasingly larger NO calculations up to  $N = 20$ . The visual inspection of the  $p_X$  vs  $1/N$  curve immediately suggests that  $p_E = 6 + A/N + \dots$  and  $p_\delta = 4 + A/N + \dots$ . The supposition has been confirmed by doing fits to the asymptotic form

$$p = p_0 + \sum_{i=1}^{N_p} \frac{p_i}{N^i}, \quad (21)$$

for increasingly larger values of  $N_p$ . The results for  $p_0$  and  $p_1$  are given in Table II. The present calculations give  $p_0$  values of 5.992, 5.997 and 5.996 (the 5-term series which gave  $p_0 = 5.967$  is likely to be more susceptible to small imperfections in the NOs). A least-squares fit to the function  $p_E = p_0 + p_1/N^t$  over the  $N \in [11, 20]$  interval gave  $p_0 = 6.0005$  and  $t = 1.070$ . A least-squares fit to the function  $p_\delta = p_0 + p_1/N^t$  over the  $N \in [11, 20]$  interval gave  $p_0 = 3.992$  and  $t = 0.9174$ . A small even-odd ripple was present in the  $p_\delta$  vs  $N$  graph.

The linear variation of  $p_X$  vs  $1/N$  indicates the asymptotic series

$$\Delta E^N = \frac{A_E}{N^6} + \frac{B_E}{N^7} + \frac{C_E}{N^8} + \dots \quad (22)$$

$$\Delta \delta^N = \frac{A_\delta}{N^4} + \frac{B_\delta}{N^5} + \frac{C_\delta}{N^6} + \dots \quad (23)$$

for the variation of the  $\Delta E^N$  and  $\Delta \delta^N$  with  $N$ . The  $O(N^{-6})$  variation of  $\Delta E^N$  has been known since the work of Carroll *et al* [1]. The present calculations give a more precise determination of the exponent. The value of  $p \approx 5.7$  previously reported by Goldman [13] can be discounted. Besides giving the leading order term with increased precision, the present calculations also demonstrate the order of the next term in the asymptotic series is  $O(N^{-7})$  and thereby strengthen the justification

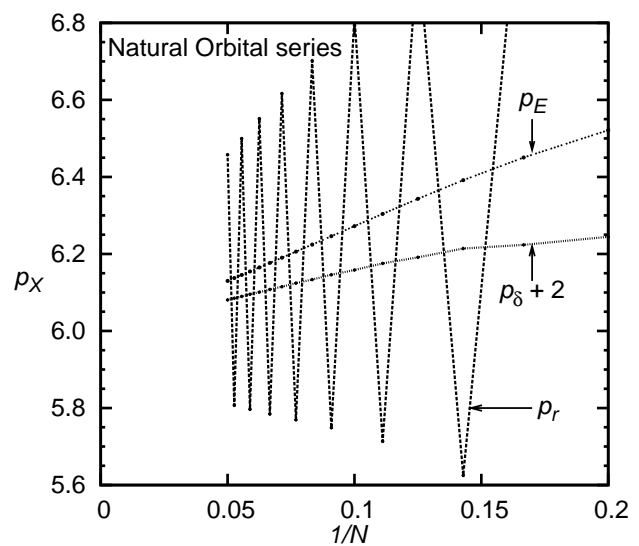


FIG. 9: The estimated exponents  $p_E$ ,  $p_\delta$  and  $p_r$  as a function of  $\frac{1}{N}$  for the NO expansion of He ground state. The value of  $p_r$  shows strong even-odd oscillations.

of asymptotic series based on expansions of the principal quantum number [12].

The best NO estimate of  $\langle E \rangle^\infty$  in Table II was about an order of magnitude less accurate than that obtained from the LTO calculation. This was not unexpected since the values of  $\langle E \rangle^N$  in Table III are not the “exact” NO energies, merely very good estimates of these energies. Also, use of the NO basis inevitably means a more complicated calculation, and so it is more likely to be affected by round-off errors and discretization errors in the numerical quadratures.

The coefficient of the leading order term for  $\Delta E$  was  $-0.2999$  hartree which is a bit larger in magnitude than the value initially given by Carroll *et al* [1], namely  $-0.24$  hartree. This level of agreement is acceptable given the fact that Carroll *et al* actually use a slightly different  $A_E/(N - 1/2)^{-6}$  functional form (and do not allow for higher order terms) and extract the value of  $A_E$  at  $N \approx 10$  which is too low to extract the asymptotic value of  $A_E$  (the value of  $A_E$  varies by more than 10% between  $N = 10$  and  $N = 20$  for a single-term asymptotic formula). The precision of the Carroll *et al* calculation is also less than that of the present calculation (they obtained  $-2.879028765$  hartree as their variational limit).

The leading order term for the variation of  $\Delta \delta^N$  with  $N$  was  $O(N^{-4})$ . This dependence is consistent with earlier work of Halkier *et al* [20] who found that the variation of  $\Delta \delta^X$  with  $X$  to be  $O(X^{-2})$  where  $X$  is the principal quantum number of the natural orbital. When analyzing this set of data it was discovered that there were regular fluctuations in the derived parameters as a function of  $N$  as the analysis was made more sophisticated. When the 3-term approximation to eq. (17) was used the value of  $p_0$  oscillated between 3.94 and 4.06 depend-

ing on whether  $N$  was even or odd (the oscillations in  $p_1$  were more marked). The oscillations became larger for the 4-term fit, here it was found that the  $p_0$  typically flipped between 3.4 and 4.6. The actual values given in Table II were obtained by weighted average, e.g.  $p_0 = 0.25p_0(N=19) + 0.50p_0(N=20) + 0.25p_0(N=21)$ .

These oscillations are most likely due to the physical properties of the basis set expansion of the He ground state. It has been known for a long time that treating the two electrons as an inner and outer electron can lead to a better description of the radial correlations [7, 27]. With the electrons having a tendency to separate into inner and outer radial orbitals the possibility does exist that achieving this separation might be slightly easier or harder if there are an even or odd number of NOs. It must be recalled that NOs themselves are objects that depend on the electron dynamics. The convergence of the mean electron-nucleus distance, i.e.  $\langle r \rangle$  was also examined and the convergence pattern was quite irregular. Defining  $p_r$  using eq. (14) results in the strongly oscillating plot of  $p_r$  vs  $1/N$  observed in Figure 9. The oscillations disappear if  $\langle r \rangle^N$  for only even  $N$  (or only odd  $N$ ) are used in a slightly modified version of eq. (14) and one finds the leading order term in  $\Delta r^N$  is  $O(N^{-6})$ . It should be noted that similar even-odd fluctuations have also been observed in high precision calculations using correlated basis sets [12, 28, 29].

TABLE III: The term by term energy and  $\langle \delta \rangle$  -function (in  $a_0^3$ ) expectation values for the NO basis.

$N$	$\langle E \rangle^N$	$\langle \delta \rangle^N$
1	-2.861 531 101 7265	0.190 249 652 529
2	-2.877 929 200 9378	0.161 369 548 453
3	-2.878 844 196 5241	0.157 747 352 993
4	-2.878 980 288 7909	0.156 661 432 897
5	-2.879 012 046 8823	0.156 240 259 959
6	-2.879 021 844 0177	0.156 045 264 861
7	-2.879 025 501 6647	0.155 943 428 536
8	-2.879 027 069 6581	0.155 885 238 797
9	-2.879 027 815 8906	0.155 849 654 582
10	-2.879 028 201 2549	0.155 826 694 126
11	-2.879 028 413 7401	0.155 811 228 411
12	-2.879 028 537 3691	0.155 800 434 791
13	-2.879 028 612 5987	0.155 792 675 857
14	-2.879 028 660 1493	0.155 786 956 341
15	-2.879 028 691 2007	0.155 782 648 350
16	-2.879 028 712 0592	0.155 779 342 132
17	-2.879 028 726 4219	0.155 776 762 792
18	-2.879 028 736 5303	0.155 774 721 119
19	-2.879 028 743 7842	0.155 773 084 071
20	-2.879 028 749 0810	0.155 771 756 198

The asymptotic behavior of the natural orbital configu-

ration coefficients were also determined. The coefficients are the  $d_i$  in eq. (20). Assuming that the  $d_i$  scale as an inverse power series,  $d_i \approx A_d/i_{\text{NO}}^p$  gives

$$p_{\text{NO}} = \ln \left( \frac{d_i^N}{d_{i-1}^N} \right) / \ln \left( \frac{i}{i-1} \right). \quad (24)$$

A fit of  $p$  to  $i$  using the formula

$$p_{\text{NO}} = p_0 + \frac{p_1}{i} + \frac{p_2}{i^2}, \quad (25)$$

gave values of  $p_0$  that ranged from 3.998 to 4.003 for successive fits to the 3 previous values for  $i$ -values between 12 and 20 for the  $\lambda_{60}$  basis. It was found that

$$d_i \approx \frac{0.362}{i^4} + \frac{0.589}{i^5} + \frac{1.492}{i^6}, \quad (26)$$

at  $i = 20$ . Carroll *et al* obtained the result  $d_i \approx \frac{0.271}{(i-1/2)^4}$  [1].

## VII. CONVERGENCE OF AN OPTIMIZED BASIS

In this section the convergence properties of the LTO basis which is energy optimized at each  $N$  are studied. Developing the sequence of exponents  $\lambda_M$  that gave the lowest energy for a LTO basis of dimension  $M$  was tedious. Defining  $\delta\langle E \rangle$  and  $\delta\langle \delta \rangle$  as the differences in  $\langle E \rangle$  and  $\langle \delta \rangle$  arising from an imprecisely known  $\lambda_M$ , one has the relations

$$\delta\langle E \rangle \approx A(\delta\lambda)^2 \quad (27)$$

$$\delta\langle \delta \rangle \approx B(\delta\lambda). \quad (28)$$

The quadratic dependence of  $\delta\langle E \rangle$  with respect to  $\delta\lambda$  does make it easier to generate the sequence of  $\langle E \rangle^N$  values. But this quadratic dependence upon  $\delta\lambda$  does make it harder to determine  $\lambda_M$  since the energy only depends weakly on  $\lambda$  in the vicinity of the minimum. Since  $\delta\langle \delta \rangle$  depends linearly on  $\delta\lambda$ , any imprecision in  $\lambda_M$  impacts the precision of the  $\langle \delta \rangle^N$  sequence more severely.

Some specific data can be used to put this in perspective. The  $\lambda_M$  for  $M = 1, \dots, 30$  have been determined to a precision for  $10^{-6}$  for the calculations reported in this section. These gave an energy that was accurate to  $10^{-18}$  hartree for the  $M = 15$  calculation, but  $\langle \delta \rangle$  was only known to a precision of  $10^{-11}$   $a_0^3$ . Determination of  $\langle \delta \rangle$  to a precision of  $10^{-15}$   $a_0^3$  would require fixing  $\lambda_M$  with an accuracy of  $10^{-10}$  which would necessitate an energy given to a accuracy of  $10^{-26}$  hartree.

The behavior of  $p_E$  and  $p_\delta$  vs  $N$  was sufficiently complicated that an initial least squares fit to the equation  $p = p_0 + p_1/N^t$  was performed for  $N \in [18, 30]$ . The results of the fit gave

$$p_E = 5.6562 + \frac{15.69}{N^{2.7326}} \quad (29)$$

$$p_\delta = 3.8093 - \frac{0.3832}{N^{0.5438}}. \quad (30)$$

The distinctive aspect about the fit is the difference in the leading terms of the inverse power series for  $p_E$  and  $p_\delta$ . Figure 10 shows that variation of  $p_E$  for the optimized LTO basis as a function of  $1/N^{2.7326}$  up to  $N = 30$ . The plot of  $p_\delta$  is tending to curl up for the smallest values of  $1/N^{2.7326}$  because it is not linear in  $1/N^{2.7326}$ .

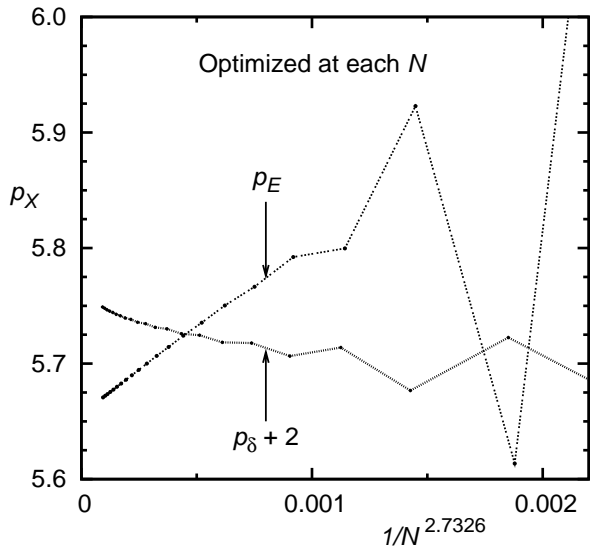


FIG. 10: The estimated exponents  $p_E$  and  $p_\delta$  as a function of  $N^{-2.7326}$  for the optimized basis. The variation of  $p_\delta$  with  $N^{-2.7326}$  is not expected to be linear.

Another notable feature of Figure 10 were the oscillations in  $p_E$  and  $p_\delta$  for even and odd values of  $N$ . Oscillations in  $p_\delta$  were previously seen for the NO sequence but the  $p_\delta$  oscillations in Figure 10 are more pronounced than those in Figure 9. Some of the values in Table II were given using the 3-point averaging used previously for the Natural Orbital sequence.

The asymptotic analysis to determine the variational limits were performed with the following series

$$\Delta E^N = \frac{A_E}{N^{5.6562}} + \frac{B_E}{N^{8.3888}} \quad (31)$$

$$\Delta \delta^N = \frac{A_\delta}{N^{3.8093}} + \frac{B_\delta}{N^{4.3531}} \quad (32)$$

The results of the analysis are given in Table II. The energy is predicted with an accuracy of  $10^{-10}$  hartree while  $\langle \delta \rangle^\infty$  is given to an accuracy of  $10^{-8} a_0^3$ . Equations (31) and (32) were not worth extending to include more terms. The power of the next term in eq. (31) is not obvious (refer to the Appendix A) and the oscillations in  $p_\delta$  to a certain extent negate the value of extending eq. (32) to include additional terms (even if we knew what those terms were!).

Results of a sequence of CI calculations of the He ground state with an  $\ell = 0$  basis have been presented. This can be regarded as the simplest model of a real atom that has a correlation cusp. The energy dependence of the LTO basis was  $\Delta E \approx O(N^{-7/2})$ . This rather slow convergence rate can be improved by fitting a succession of  $\langle E \rangle^N$  values to the inverse power series  $\Delta E^J = A_E/N^{-7/2} + B_E/N^{-8/2} + \dots$  and estimating the  $N \rightarrow \infty$  limit. It ultimately proved possible after adopting quadruple precision arithmetic, to reproduce the known energy in this model to an accuracy of  $1 \times 10^{-14}$  hartree. The specific choice of the asymptotic series should be regarded as conjecture supported by numerical evidence. More definite proof would require the calculations to be extended to  $N > 100$ . The common exponent of the LTO basis should not be chosen to optimize the energy for the largest calculation since this results in a distorted convergence pattern. In effect, optimizing the LTO exponent for  $N$  LTOs, and then using the  $(N-3)$ ,  $(N-2)$ ,  $(N-1)$  and  $N$  energies to determine the coefficients of a 3-term expansion to eq. (18) will give an inaccurate estimate of the energy correction needed to achieve the variational limit. Any extrapolation would seem to require that  $N$  (the number of LTOs) should exceed  $M$  (the basis dimension at which  $\lambda$  was optimized) by about ten or more. This conclusion holds for both the energy and electron-electron  $\delta$ -function. The very slow  $O(1/N^{5/2})$  convergence of  $\langle \delta \rangle$  was also circumvented by the use of the  $N \rightarrow \infty$  corrections.

The examinations of the convergence rate for an NO basis set revealed a faster convergence. The NO basis converged as  $O(N^{-6})$  with the next term being  $O(N^{-7})$ . The present determinations of the convergence rates are more rigorous than those of Carroll *et al* [1]. One surprising result was the slight even-odd oscillation in the convergence of the inter-electronic  $\delta$ -function. Examination of the  $\langle r \rangle$  revealed noticeable even-odd oscillations in  $p_r$ . The presence of these ripples could complicate determination of the variational limit of expectation values other than the energy. It was possible to extrapolate the energy of a 20 orbital NO basis to the variational limit with an accuracy of about  $10^{-12}$  hartree.

The convergence rate of the optimized LTO basis was  $O(N^{-5.6562})$  with the next term being  $O(N^{-8.3888})$ . The degree of uncertainty in both of these exponents is much larger than for the fixed  $\lambda$  LTO sequence or the NO sequence. The extremely tedious nature of the  $\lambda$  optimization, combined with the lack of knowledge about the nature of the asymptotic series beyond the first two terms, make this extrapolation a less attractive proposition. The noticeable even-odd oscillation in  $p_\delta$  and even  $p_E$  further render the method even more unattractive. The implications of this behavior are not confined to the present work. For example, it is likely that correlated

exponential basis sets composed of functions with

$$\xi(r_1, r_2, r_{12}) = r_1^i r_2^j r_{12}^m \exp(-\lambda r_1) \exp(-\lambda r_2) \quad (33)$$

could also exhibit complicated convergence patterns since  $\lambda$  is often energy optimized as the basis dimension is increased in size [30]. Consequently, it would not be surprising for estimates of the  $N \rightarrow \infty$  energy correction for variational calculations on systems using a Hylleraas basis to be unreliable. For example, Yan and coworkers have estimated the variational limit in a high precision calculation of PsH using a Hylleraas type basis [31]. Their estimated energy correction for the PsH ground state energy (only  $9.6 \times 10^{-8}$  hartree) was too small by at least a factor of three [32].

One of the main motivations for the present study was to gain insight into solving the problems associated with the very slow convergence of CI calculations for mixed electron-positron systems [15, 17, 23, 33]. In effect, the problem is to determine the complete basis set limit [12, 34, 35] for these exotic systems. The slow  $O(N^{-7/2})$  convergence of the energy for an LTO basis set is greatly improved by the adoption of extrapolation schemes. Using the  $N = 10$  energy for the  $\lambda_{10}$  basis and the best extrapolation of the  $N = 60$  calculation in Table II as two reference points, one deduces an effective convergence rate of  $O(N^{-10})$ . The penalty associated with the use of the extrapolation formulae is the necessity to use quadruple precision arithmetic if 3 or more terms are retained in the inverse power series (note, a 3-term series for  $\Delta\delta^N$  was numerically stable in double precision arithmetic). The need to use the quadruple precision arithmetic is caused by the very small size of the  $\Delta E^N$  increments and the impact of round-off error on the fit to the inverse power series. One somewhat ironic feature is that it is necessary to use a basis that is *not* energy optimized so that the extrapolation to the variational limit can be done reliably.

### Acknowledgments

The authors would like to thank Shane Caple and Roy Pidgeon of CDU for providing access to extra computing resources. We would also like to thank David Bosci of Hewlett-Packard(Darwin) for giving us access to a demonstration Itanium workstation.

### APPENDIX A: ANALYSIS OF THE $p$ -DEPENDENCE

Let us demonstrate that an asymptotic series

$$\Delta X^N = \frac{A}{N^q} + \frac{B}{N^{q+t}} \dots = \frac{A}{N^q} \left( 1 + \frac{C}{N^t} \dots \right) \quad (A1)$$

(with  $C = B/A$ ) leads to  $p = q + F/N^t$  when  $p$  is defined from successive  $\Delta X^N$  increments by

$$p = \ln \left( \frac{\Delta X^{N-1}}{\Delta X^N} \right) / \ln \left( \frac{N}{N-1} \right). \quad (A2)$$

Substituting  $\Delta X^N$  and  $\Delta X^{N-1}$  from eq. (A1) gives

$$p = \ln \left( \frac{\frac{A}{(N-1)^q} \left( 1 + \frac{B}{(N-1)^t} \right)}{\frac{A}{N^q} \left( 1 + \frac{B}{N^t} \right)} \right) / \ln \left( \frac{N}{N-1} \right). \quad (A3)$$

The logarithm in the numerator can be split into two terms

$$\ln \left( \frac{\Delta X^{N-1}}{\Delta X^N} \right) = q \ln \left( \frac{N}{N-1} \right) + \ln \left( \frac{1 + \frac{C}{(N-1)^t}}{1 + \frac{C}{N^t}} \right) \quad (A4)$$

The first term conveniently cancels with the denominator to give  $q$ . The argument of the second term can be expanded

$$\begin{aligned} \frac{1 + \frac{C}{(N-1)^t}}{1 + \frac{C}{N^t}} &\approx \left( 1 + \frac{C}{N^t} + \frac{tC}{N^{t+1}} \right) \left( 1 - \frac{C}{N^t} + \frac{C^2}{N^{2t}} \right) \\ &\approx 1 + \frac{tC}{N^{t+1}} + \dots \end{aligned} \quad (A5)$$

Using  $\ln(1+x) \approx x$  leads to

$$\ln \left( \frac{1 + \frac{C}{(N-1)^t}}{1 + \frac{C}{N^t}} \right) \approx \frac{tC}{N^{t+1}}. \quad (A6)$$

The denominator is simplified using  $\ln(N/(N-1)) = \ln(1 + 1/(N-1)) \approx 1/N$  to finally give

$$p = q + \frac{tC}{N^t} + \dots \quad (A7)$$

as required. If eq. (A1) has successive terms where the power increments by  $t = 1$  or  $t = 1/2$  indefinitely, then this leads to a corresponding series, eq. (A7) that also have powers that respectively increment by 1 or 1/2 indefinitely. This is not necessarily true for arbitrary  $t$  in eq. (A1).

### APPENDIX B: SCALING OF THE 2-ELECTRON INTEGRALS

The most time-consuming part of the calculation was the generation of the electron-electron and annihilation matrix elements. However, the expense of this was greatly reduced by generating an initial set of integrals for a given  $\lambda$ , and then using a scaling factor to generate the integral lists for other values of  $\lambda$ .

The basic integral that has to be done is

$$\begin{aligned} R(n_a, n_b, n_c, n_d, \lambda) &= \iint dr_1 dr_2 N_a(\lambda) N_b(\lambda) \\ &\times N_c(\lambda) N_d(\lambda) f_a(\lambda r_1) f_b(\lambda r_2) \\ &\times V(r_1, r_2) f_c(\lambda r_1) f_d(\lambda r_2) \end{aligned} \quad (B1)$$

All integrals can be defined in terms of  $R(n_a, n_b, n_c, n_d, \lambda = 1)$ . Consider the integral (B1) and make the transformation  $\lambda r = u$ . Therefore  $r_1 = u_1/\lambda$  and  $r_2 = u_2/\lambda$ . Similarly  $dr_1 = du_1/\lambda$  and  $dr_2 = du_2/\lambda$  and therefore

$$R(n_a, n_b, n_c, n_d, \lambda) = \frac{1}{\lambda^2} \iint du_1 du_2 N_a(\lambda) N_b(\lambda) \times N_c(\lambda) N_d(\lambda) f_a(u_1) f_b(u_2) \times V(r_1, r_2) f_c(u_1) f_d(u_2) \quad (\text{B2})$$

From eq. (9),  $N_a(\lambda) = \lambda^{1/2} N_a(\lambda = 1)$ , so

$$R(n_a, n_b, n_c, n_d, \lambda) = \iint du_1 du_2 N_a(1) N_b(1) \times N_c(1) N_d(1) f_a(u_1) f_b(u_2) \times V(r_1, r_2) f_c(u_1) f_d(u_2) \quad (\text{B3})$$

The scaling for the electron-electron repulsion integral is  $|\mathbf{r}_1 - \mathbf{r}_2|^{-1} = \lambda |\mathbf{u}_1 - \mathbf{u}_2|^{-1}$ . Hence

$$R(n_a, n_b, n_c, n_d, \lambda) = \lambda R(n_a, n_b, n_c, n_d, 1), \quad (\text{B4})$$

for the electron-electron integral. When the operator is the  $\delta$ -function, one uses the result  $\delta(\mathbf{r}_1 - \mathbf{r}_2) = \lambda \delta(\mathbf{u}_1 - \mathbf{u}_2)$  to give

$$R(n_a, n_b, n_c, n_d, \lambda) = \lambda R(n_a, n_b, n_c, n_d, 1). \quad (\text{B5})$$

- 
- [1] D. P. Carroll, H. J. Silverstone, and R. P. Metzger, *J. Chem. Phys.* **71**, 4142 (1979).  
[2] R. N. Hill, *J. Chem. Phys.* **83**, 1173 (1985).  
[3] W. Kutzelnigg and J. D. Morgan III, *J. Chem. Phys.* **96**, 4484 (1992).  
[4] P. Decleva, A. Lisini, and M. Venuti, *Int. J. Quantum Chem.* **56**, 27 (1995).  
[5] O. Jitrik and C. Bunge, *Phys. Rev. A* **56**, 2614 (1997).  
[6] E. Ottoschowski and W. Kutzelnigg, *J. Chem. Phys.* **106**, 6634 (1997).  
[7] J. S. Sims and S. A. Hagstrom, *Int. J. Quantum Chem.* **90**, 1600 (2002).  
[8] M. W. J. Bromley and J. Mitroy, *Int. J. Quantum Chem.* p. under review (2006).  
[9] C. Schwartz, *Phys. Rev.* **126**, 1015 (1962).  
[10] W. Kutzelnigg, *Int. J. Quantum Chem.* **31**, 467 (1994).  
[11] P. O. Löwdin and H. Shull, *Phys. Rev. A* **101**, 1730 (1956).  
[12] W. Klopper, K. L. Bak, P. Jorgensen, J. Olsen, and T. Helgaker, *J. Phys. B* **32**, R103 (1999).  
[13] S. P. Goldman, *Phys. Rev. A* **52**, 3718 (1995).  
[14] H. Shull and P. O. Löwdin, *J. Chem. Phys.* **23**, 1362 (1955).  
[15] M. W. J. Bromley and J. Mitroy, *Phys. Rev. A* **65**, 012505 (2002).  
[16] E. Holoien, *Phys. Rev.* **104**, 1301 (1956).  
[17] J. Mitroy and M. W. J. Bromley, *Phys. Rev. A* **73**, 052712 (2006).  
[18] W. Kutzelnigg and P. von Herigonte, *Adv. Quant. Chem.* **36**, 185 (1999).  
[19] S. P. Goldman, *Phys. Rev. A* **40**, 1185 (1989).  
[20] A. Halkier, T. Helgaker, W. Klopper, and J. Olsen, *Chem. Phys. Lett.* **319**, 287 (2000).  
[21] J. Mitroy, M. W. J. Bromley, and G. G. Ryzhikh, *J. Phys. B* **35**, R81 (2002).  
[22] M. Abramowitz and I. E. Stegun, eds., *Handbook of Mathematical Functions* (US GPO, Washington DC, 1972), Natl. Bur. Stand. Appl. Math. Ser. 55.  
[23] M. W. J. Bromley and J. Mitroy, *Phys. Rev. A* **65**, 062505 (2002).  
[24] S. P. Goldman, *Phys. Rev. Lett.* **73**, 2547 (1994).  
[25] C. Bunge, *Theor. Chima. Acta* **16**, 126 (1970).  
[26] M. W. J. Bromley and J. Mitroy, *Phys. Rev. A* **66**, 062504 (2002).  
[27] H. Shull and P. O. Löwdin, *J. Chem. Phys.* **25**, 1305 (1956).  
[28] B. Schiff, H. Lifson, C. L. Pekeris, and P. Rabinowitz, *Phys. Rev.* **140**, A1104 (1965).  
[29] G. W. F. Drake, *Phys. Scr.* **T83**, 83 (1999).  
[30] Z. C. Yan, p. (unpublished) (????).  
[31] Z. C. Yan and Y. K. Ho, *Phys. Rev. A* **59**, 2697 (1999).  
[32] J. Mitroy, *Phys. Rev. A* **73**, 054502 (2006).  
[33] J. Mitroy and I. A. Ivanov, *Phys. Rev. A* **65**, 042705 (2002).  
[34] G. A. Petersson, D. K. Malick, W. G. Wilson, J. W. Ochterski, J. A. Montgomery, and M. J. Frisch, *J. Chem. Phys.* **109**, 10570 (1988).  
[35] G. Tarczay, A. G. Csazar, W. Klopper, V. Szalay, W. D. Allen, and H. F. Schaefer III, *J. Chem. Phys.* **110**, 11971 (1999).